

Numerical Simulation of Turbulent Flow and Heat Transfer in a B-Type Section Pipe with Porous Bottom Wall

M. Khayat*

Department of Mechanical and Aerospace Engineering,
Science and Research Branch, Islamic Azad University, Tehran, Iran
E-mail: mkhayat@srbiau.ac.ir

*Corresponding author

R. Aliabbasi

Department of Mechanical and Aerospace Engineering,
Science and Research Branch, Islamic Azad University, Tehran, Iran
E-mail: Abbasi.65@gmail.com

M. Taeibi Rahni

Department of Mechanical and Aerospace Engineering,
Science and Research Branch, Islamic Azad University, Tehran, Iran
E-mail: taeibi@sharif.edu

Received: 4 Mars 2012, Revised: 26 June 2012, Accepted: 29 July 2012

Abstract: In this work, three-dimensional turbulent forced convection flow through a B-Type section pipe, with porous material is inserted at the bottom wall, is investigated numerically. The B-Type section pipe is used in cooling systems, such as cars' radiator. The main purpose of this research is to enhance heat transfer and to reduce the scales of such systems. The governing equations are formulated according to the volume averaging method. The results are verified by comparing them with some valid numerical data. The dependence of the Nusselt number and pressure drop on the porosity, permeability and Reynolds number are investigated. The results indicate that, at the maximum flow rate, the heat transfer can be enhanced about 8 times by using porous material while the pressure drop is increased about 2.5 times.

Keywords: B-Type Section, Forced Convection, Porous Media, Turbulent Flow

Reference: Khayat, M., Aliabbasi, R., and Taeibi Rahni, M., "Numerical simulation of turbulent flow and heat transfer in a B-Type section pipe with porous bottom wall", Int J of Advanced Design and Manufacturing Technology, Vol. 5/No. 5, 2012, pp. 61-69.

Biographical notes: **M. Khayat** received his PhD in Mechanical Engineering from Sharif University, in 2007. He is currently Assistant Professor at the Department of Mechanical and Aerospace Engineering, University of IAU, Science and Research Branch, Tehran, Iran. His current research interest includes fluid mechanics, thermodynamics and heat transfer. **R. Aliabbasi** is MSc student of mechanical engineering at the University of IAU, Science and Research Branch, Tehran, Iran. His current research focuses on fluid mechanics and heat transfer in the porous media. **M. Taeibi Rahni** received his PhD in Aerospace Engineering from the University of Illinois in 1995. He is currently Associate Professor Sharif University of Technology and at the Department of Mechanical and Aerospace Engineering, University of IAU, Science and Research Branch, Tehran, Iran.

1 INTRODUCTION

An important issue in thermal power engineering is the development of compact and highly efficient heat exchangers which are made of porous materials with high heat conductivity. Flows through a porous medium in a channel has practical applications such as heat exchangers, electronic component cooling systems, thermal insulation, nuclear reactors, drying processes, and so on. The forced convective flow through porous media was studied by many investigators in several cases with various procedures: analytically, numerically and experimentally.

Aliabbasi et al. simulated turbulent flow and heat transfer in a flattened tube partially and completely filled with a porous material [1]. Yang and Hwang carried out Numerical simulations to investigate the turbulent heat transfer enhancement in the pipe filled with porous media [2]. Braga and de Lemos presented numerical computations for laminar and turbulent natural convection within a horizontal cylindrical annulus filled with a fluid saturated porous medium [3]. Li et al. studied numerically fluid flow and heat-transfer characteristics in a channel with staggered porous blocks [4]. Akansu presented a numerical heat transfer and pressure drop for porous rings inserted in a pipe with constant applied heat flux to the outer surface of the pipe [5].

Pavel and Mohammad investigated the effect of metallic porous materials, inserted in a pipe, on the rate of heat transfer while the pipe is subjected to a constant and uniform heat flux [6]. Kaviany studied laminar flow through a porous channel bounded by two parallel plates maintained at constant and equal temperatures, but this study is limited to the situation in which fluid and solid phases are in local thermal equilibrium [7]. Alkam and Al-Nimr introduced a novel method to improve the thermal performance of a conventional concentric tube heat exchanger by emplacing porous substrates at both sides of the inner tube wall [8]. Tada and Ichimiya studied theoretically the thermal development of forced convection using a circular tube filled with a saturated porous medium, with constant wall heat flux, and with the effect of viscous dissipation [9].

Marafie and Vafai investigated analytically forced convective flow through a channel filled with a porous medium [10]. Khaled and Vafai studied numerically forced convective heat transfer inside channels by controlling thermal dispersion effects inside the fluid [11]. Mohamad studied numerically the flow in a pipe or channel fully or partially filled with a porous medium. An air stream with a uniform velocity and

temperature is considered at the inlet to the conduit [12]. Macedo and et al. studied The influence of turbulent effects on a fluid flow through a (pseudo) porous media by numerically solving the set of Reynolds-Averaged Navier-Stokes equations [13]. Silva and de Lemos presented numerical solutions for laminar and turbulent flow in a channel partially filled with a flat layer of porous material [14], [15].

In the present study, a B-Type section channel, with a porous wall that a uniform heat flux is applied on all of the walls is under consideration. B-Type Section pipes due to of their specific geometry, accelerate the turbulence and improve the heat transfer. To perform a detailed study of the hydrodynamic and heat transfer characteristics within these types of channels, the finite volume method for a steady-state, incompressible, and three-dimensional flow is employed.

2 MATHEMATICAL MODEL

2.1. Geometry

A schematic diagram for the problem under consideration is shown in Fig. 1, which gives the geometry of a B-Type section pipe with a porous wall. The total length of the pipe is 600 mm and in order to have a reasonable pressure drop, the thickness of the porous layer, 0.1 times the hydraulic radius of the pipe is considered. A uniform heat flux of 50 kW/m^2 is applied to the outer surface of the pipe walls. The natural and radiation modes of heat transfer are assumed to be negligible due to the high flow rates.

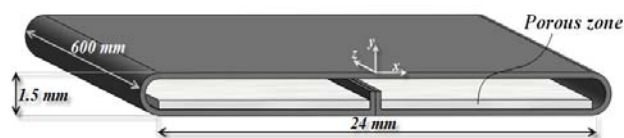


Fig. 1 Schematic configuration of the physical model

2.2. governing equations

A macroscopic form of the governing equations in the porous medium is obtained by taking the volumetric average of the entire Navier–Stokes equation set combined with a $k-\epsilon$ turbulence model. In this development, the porous medium is considered to be rigid and saturated by the incompressible fluid. The macroscopic continuity equation is given by Eq. (1).

$$\nabla \cdot (\gamma \rho \vec{v}) = 0 \quad (1)$$

where ‘ γ ’ is the porosity of porous medium. The macroscopic momentum equation for an incompressible fluid in the porous medium can be written as Eq. (2).

$$\nabla \cdot (\gamma \rho \bar{v}) = -\gamma \nabla P + \nabla \cdot (\gamma \bar{\tau}) - \left(\frac{\mu}{\alpha} + \frac{C_2 \rho}{2} |\bar{v}| \right) \bar{v} \quad (2)$$

where ‘ μ ’ is the fluid dynamic viscosity, ‘ α ’ is the permeability, ‘ C_2 ’ is known in the literature as the non-linear Forchheimer term or inertia coefficient, and the last two terms in Eq. (2) represent the time-mean total drag per unit volume, acting on the fluid by the action of the porous structure. The permeability, ‘ α ’, and the inertia coefficient, ‘ C_2 ’, are evaluated by using the following empirical correlations:

$$\alpha = \frac{\gamma^3 d_p^2}{150(1-\gamma)^2} \quad (3)$$

$$C_2 = \frac{3.5}{\sqrt{150\alpha} \cdot \gamma^{3/2}} \quad (4)$$

where ‘ d_p ’ is the mean particle-diameter of porous medium.

Macroscopic equations for k and ε

Transport equations for turbulence kinetic energy, k, and its dissipation rate, ε, in porous media are reviewed by Pedras and de Lemos [16] that in our notation can be written:

$$\nabla \cdot (\rho k \bar{v}) = \nabla \cdot \left[\left(\mu + \frac{\mu_t}{\sigma_k} \right) \nabla (\gamma k) \right] + \gamma G_k - \rho \gamma \varepsilon + \gamma S_k \quad (5)$$

$$\nabla \cdot (\rho \varepsilon \bar{v}) = \nabla \cdot \left[\left(\mu + \frac{\mu_t}{\sigma_\varepsilon} \right) \nabla (\gamma \varepsilon) \right] + C_{1\varepsilon} \gamma \frac{\varepsilon}{k} (G_k) - C_{2\varepsilon} \gamma \rho \frac{\varepsilon^2}{k} + \gamma S_\varepsilon \quad (6)$$

where

$$S_k = c_k \rho \frac{\gamma k |\bar{v}|}{\sqrt{\alpha}} \quad (7)$$

$$S_\varepsilon = c_\varepsilon C_{2\varepsilon} \rho \frac{\gamma \varepsilon |\bar{v}|}{\sqrt{\alpha}} \quad (8)$$

where the ‘ $C_{1\varepsilon}$ ’ and ‘ $C_{2\varepsilon}$ ’ are constants, ‘ σ_k ’ and ‘ σ_ε ’ are the turbulent Prandtl numbers for k and ε, respectively. ‘ G_k ’ represents the production rate of turbulence kinetic energy due to the mean velocity gradients and ‘ S_k ’ is the generation rate of turbulence kinetic energy due to the action of the porous matrix. We add up ‘ S_k ’ and ‘ S_ε ’ as a source terms by using UDF (User Defined Function) in fluent software.

Modeling the Turbulent Viscosity

The turbulent (or eddy) viscosity, ‘ μ_t ’, is computed by combining ‘k’ and ‘ε’ as follows:

$$\mu_t = \rho C_\mu \frac{k^2}{\varepsilon} \quad (9)$$

Model Constants

The below values are used for the constants appearing in the previous equations:

$$C_{1\varepsilon} = 1.44, C_{2\varepsilon} = 1.92, C_\mu = 0.09, \sigma_k = 1.0, \sigma_\varepsilon = 1.3$$

Macroscopic energy equations

For the energy equation, two different models can be employed. These are the local thermal equilibrium (LTE) and local thermal non-equilibrium (LTNE) models. The descriptions of the two models are available in the work of Kaviany [17]. For large values of ‘ K_{eff}/K_f ’, the LTNE model may be required. In this study we make the assumption that the value of ‘ K_{eff}/K_f ’ is small enough by using the (AISI304) as a porous material with $K_s = 15.2 \text{ (w.m}^{-1} \cdot \text{k}^{-1})$. So we can use the LTE condition. By using the LTE model, the energy equation in the porous and open regions can be written as Eq. (10).

$$\nabla \cdot (\bar{v} (\rho_f E_f + p)) = \nabla \cdot (k_{eff} \nabla T) \quad (10)$$

$$K_{eff} = \gamma K_f + (1-\gamma) K_s \quad (11)$$

where ‘ K_f ’ is the fluid thermal conductivity and ‘ K_s ’ is the solid thermal conductivity. Because of the local equilibrium between fluid and solid phases in porous media, we have:

$$T_s = T_f = T \quad (12)$$

Calculation of heat-transfer and pressure drop

In this study, the heat convection coefficient and Nusselt number are calculated as Follows:

$$h(z) = \frac{q''}{T_{wall(ave)}(z) - T_{bulk}(z)} \quad (13)$$

where:

$$T_{wall(ave)} = \frac{1}{x} \int_0^x T(x) dx \quad (14)$$

$$T_{bulk} = \frac{\int_A T |\rho v| dA}{\int_A |\rho v| dA} \quad (15)$$

$$Nu(z) = \frac{h(z) D_h}{k} \quad (16)$$

' D_h ' is the hydraulic diameter of the pipe and 'k' is thermal conductivity of a fluid.

2.3. Boundary conditions

The boundary conditions for the configuration considered are as follows:

- The velocity u and temperature T are uniform over the cross section of the inlet boundary.
- Atmospheric pressure is assumed to occur at the exit boundary.
- No slip condition occurs on all of the walls and a uniform heat flux is applied to the outer surface of the pipe walls.
- Continuity of velocity, fluid pressure, statistical variables and their fluxes across the interface of fluid and porous medium is assumed.

2.4. Physical conditions

A free-stream flow, with a uniform temperature of 300 'K' and 'a' uniform velocity of 0.52, 0.8668, 1.387 and 1.7337 (m/s) is applied to the inlet plane. These values are calculated from different flow rate using in car radiator, namely 75, 125, 200 and 250 (L/hr) respectively, while the Reynolds numbers are: 5060, 4050, 2530 and 1520.

Table 1 indicates a range of fluid and solid phase thermo-physical properties that are used in this

investigation. The properties are not expected to be very sensitive to the variation in temperature.

Table 1 Thermo-physical Properties of used materials

	ρ , kg.m ⁻³	C_p , j.kg ⁻¹ .k ⁻¹	k w.m ⁻¹ .k ⁻¹	μ , kg.m ⁻¹ .s ⁻¹
Water (liquid)	998	4182	0.6	0.001003
AISI304 (porous)	7900	485	15.2	-----

3 NUMERICAL PROCEDURE

The governing equations with the associated boundary conditions are solved numerically utilizing a finite volume method by use of the Fluent CFD code. An optimized mesh is applied to the computational domain, with a refined mesh density in the regions near the wall boundaries. Second-order upwind method is used to model the interaction between the convection and the diffusion terms in governing equations. Also an iterative procedure based on the simple algorithm is used to deal with the linkage between pressure and velocity in the momentum equations, and temperature in the energy equation. In order to model the turbulence effects, Pedras and de Lemos [15] 'k-ε' turbulence model is used by adding UDF in fluent code. The enhanced wall treatment approach is utilized to determine the boundary conditions for the 'k' and 'ε'.

3.1. Validation of numerical method

In order to validate the numerical method, the numerical results of fully developed velocity profiles for two different porous radius ratios, are compared with the relevant cases reported by Silva and de Lemos [16]. They studied the problem of turbulent flow in a pipe fully or partially filled with porous inserted at the core of the conduit (Fig. 2). Figure 3 shows the comparison of numerical predictions of velocity profiles between present results and their numerical results for $Re=3 \times 10^5$, $Da = 10^{-4}$ and $\gamma=0.5$. It can be seen that there is a very good agreement between them.

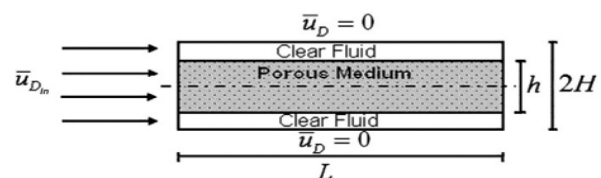


Fig. 2 Schematic configuration of the physical model which investigated by Silva and de Lemos[16]

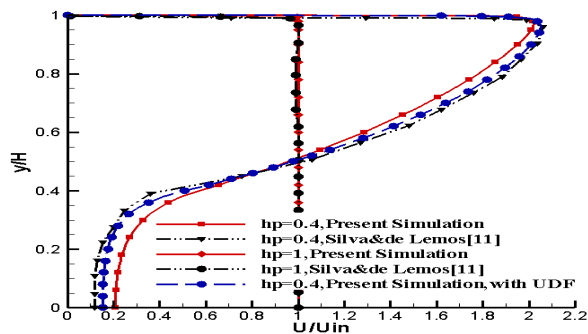


Fig. 3 Comparison of numerical predictions of velocity profiles between present results and Silva and de Lemos’s numerical results [16]

3.2. Grid independence study

In order to insure that the results are grid size independent, different meshes are tested namely 367800, 481500, 676599, 828000. From Fig. 4 it can be seen that the total cell number of 676599 is suitable for this study. Fig. 5 shows a view of mesh pattern in the cross section of the pipe.

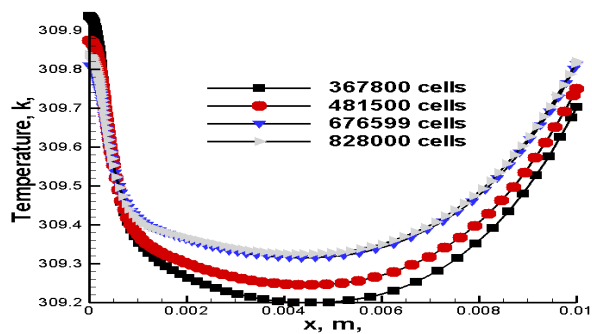


Fig. 4 Effect of grid size on temperature field for $Re \approx 5000$, $Da = 1e-3$, $\gamma = 0.7$

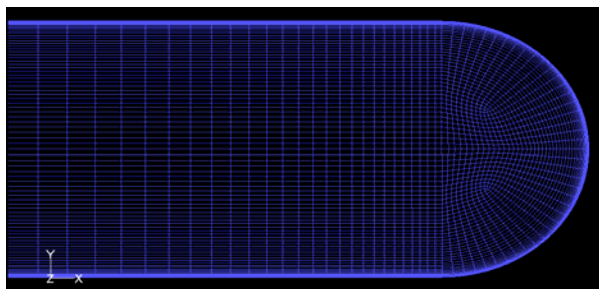


Fig. 5 A view of mesh pattern for part of the cross section of the pipe

4 RESULTS AND DISCUSSION

The turbulent flow in a B-Type section pipe partially filled with porous medium, was considered numerically for a constant heat flux boundary conditions and following results were obtained.

Figure 6 shows the velocity contours of the fully developed turbulent flow for three different Darcy numbers. The Darcy number is a dimensionless parameter for describing the fluid dynamics in a porous medium. It is directly related to the permeability of the medium. The permeability ‘ α ’ is the measure of the flow conductance of the material. It is a representation of the ability for a material to transmit the fluid. As seen from this figure, the velocity increases in the clear region especially near the upper wall as Darcy number decreases. This is due to the fact that the fluid escapes from the porous region to the clear region.

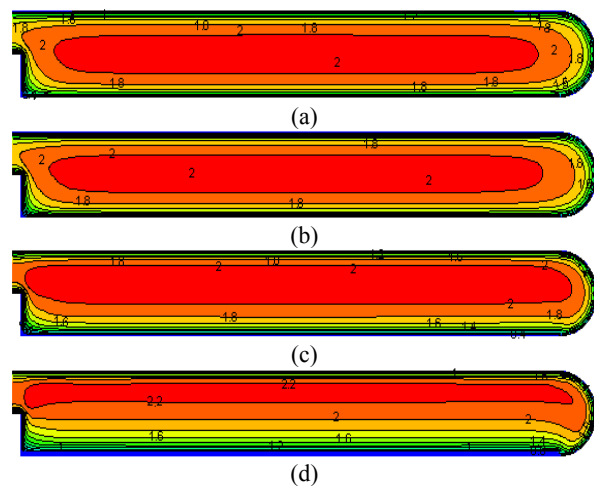


Fig. 6 Velocity contours for fully developed flow at $Re=5000$, a) without porous material or $Da \rightarrow \infty$, b) $Da=1$, $\gamma=0.98$, c) $Da=1e-3$, $\gamma=0.98$, d) $Da=1e-6$, $\gamma=0.98$

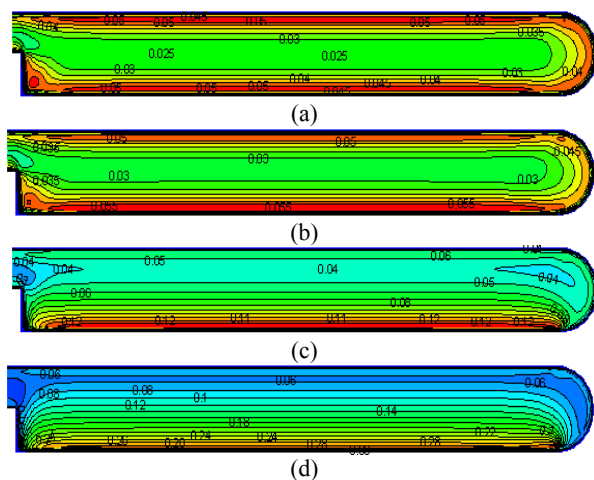


Fig. 7 Turbulence kinetic energy contours for fully developed flow at $Re=5000$, a) without porous material or $Da \rightarrow \infty$, b) $Da=1$, $\gamma=0.98$, c) $Da=1e-3$, $\gamma=0.98$, d) $Da=1e-6$, $\gamma=0.98$

Figure 7 presents contours of turbulent kinetic energy. It can be seen that large amount of turbulence is

concentrated near the bottom wall of the channel, because as the fluid permeates the porous medium, most of the mean mechanical energy of the flow is transformed into turbulence and therefore turbulent kinetic energy is generated near and inside the porous medium. Figure 8 shows the velocity profile of the turbulent flow for different Reynolds numbers where no porous material is attached to the bottom wall. It should be mentioned that increasing Reynolds number, results in higher heat transfer rates. This is due to the fact that the velocity gradient near the walls increases with increasing the Reynolds number and therefore according to the Reynolds analogy, the rate of the heat transfer increases.

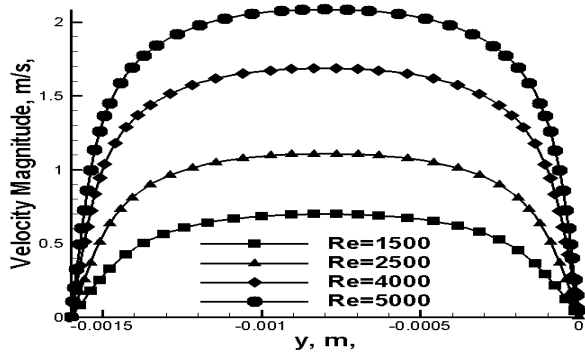


Fig. 8 Velocity profile versus y for different Reynolds numbers (without porous material)

Figure 9 shows the velocity profile of the turbulent flow for different Darcy numbers. From this figure it is readily seen that the velocity decreased in the porous region as Darcy increases. In other words, the mass flow rate decreases in the porous region as Darcy increases. This is due to the fact that the fluid escapes from the high resistance region (porous region) to the clear region.

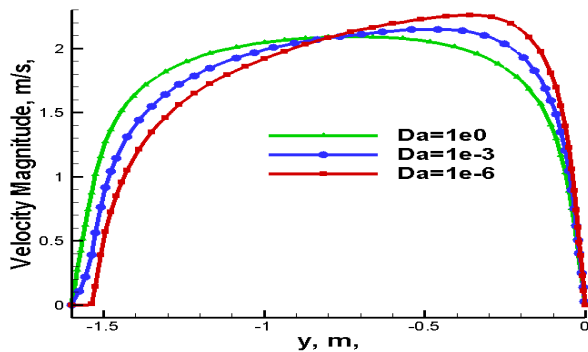


Fig. 9 Velocity profile versus y for bottom wall for different Darcy numbers ($\gamma=0.5$, $Re \approx 5000$)

The numerical predictions of temperature distributions as a function of porosities for various Reynolds

numbers namely 1500, 2500, 4000, 5000 are shown in the Figs. 10, 11, 12, and 13 respectively. It can be seen from the temperature profiles that the bottom wall temperature is least for the case with low porosity material inserts at a given Reynolds number. Also the temperature for the bottom surface decreases with an increase in porosity; it is clear that when the average wall temperature decreases, it means that the heat transfer rate increases. Because low porosities, increases the effective thermal conductivity and consequently improves the heat transfer rate.

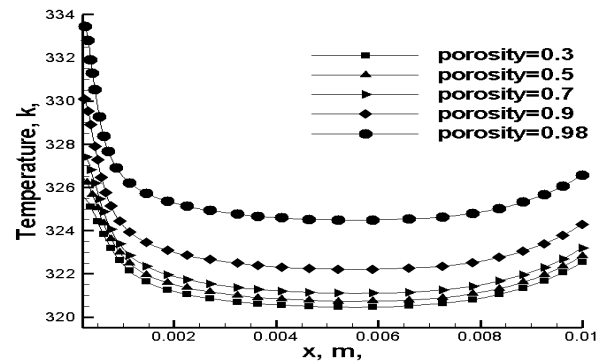


Fig. 10 Temperature profile versus x for bottom wall for different porosities ($Da=1e-3$, $Re \approx 1500$)

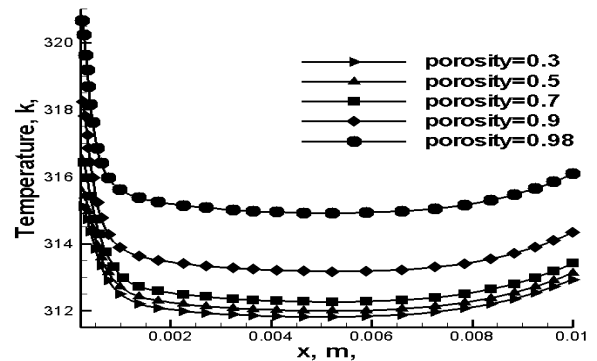


Fig. 11 Temperature profile versus x for bottom wall for different porosities ($Da=1e-3$, $Re \approx 2500$)

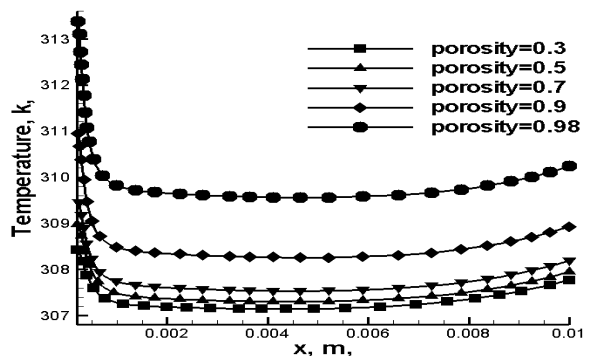


Fig. 12 Temperature profile versus x for bottom wall for different porosities ($Da=1e-3$, $Re \approx 4000$)

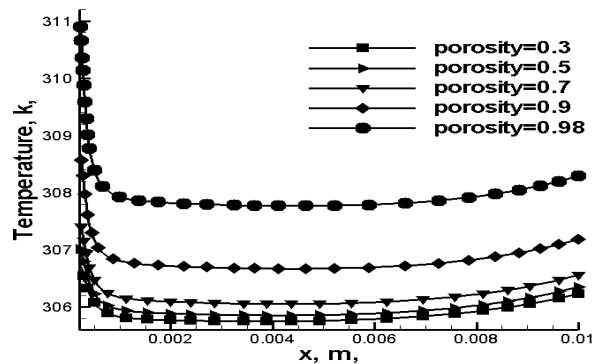


Fig. 13 Temperature profile versus x for bottom wall for different porosities ($Da=1e-3$, $Re\approx 5000$)

Figure 14 compares temperature distributions for three different Darcy numbers. From this Figure it can be seen that as Darcy number increased, the temperature of bottom wall increases and then heat transfer reduces. Because the effect of Darcy number on the fluid flow is the same as the porosity.

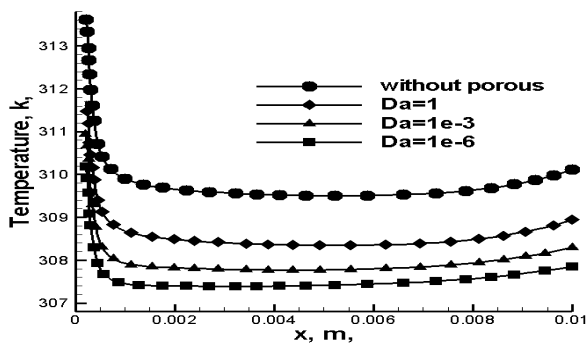


Fig. 14 Temperature profile versus x for bottom wall for different Darcy numbers ($\gamma=0.98$, $Re\approx 5000$)

The temperature distributions for different Reynolds numbers are shown in the Fig. 15. It is observed that the wall temperature decreases as Reynolds number increases and this means that heat transfer rate increases with Reynolds number. Because as the Reynolds number increases the velocity gradient near the walls increases.

Figures 16 and 17 show the variation of Nusselt number on the heated bottom wall, with porosity, for two different Darcy numbers. Using porous substrate of high thermal conductivity, improves the heat transfer from the boundaries by allowing more heat flow to be conducted to the fluid flow. It is clear from these figures that as porosity increases, its effect is vanished and the duct behaves as a clear duct, but small porosities or large values of inertial coefficient, increases the effective thermal conductivity and consequently improves the heat transfer rate. Also numerical results demonstrated that the local Nusselt number became stronger as Reynolds number increased.

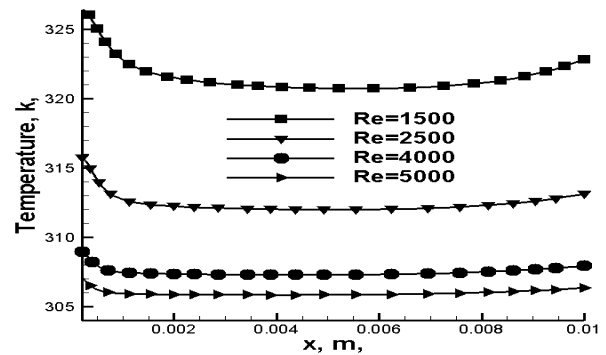


Fig. 15 Temperature profile versus x for bottom wall for different Reynolds numbers ($Da=1e-3$)

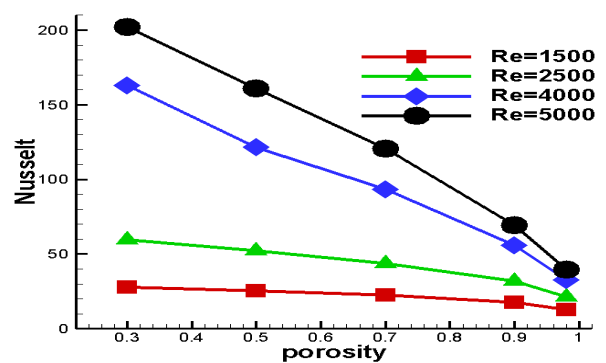


Fig. 16 Nusselt number versus porosity for different Reynolds numbers ($Da=1e-3$)

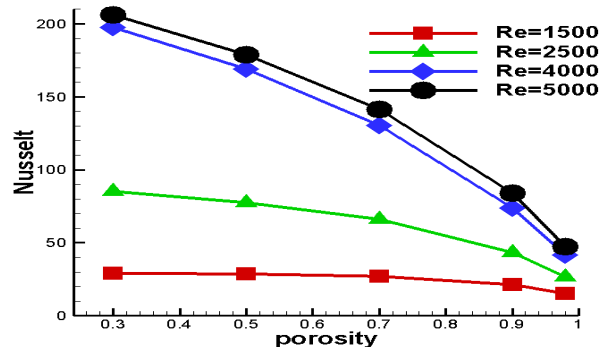


Fig. 17 Nusselt number versus porosity for different Reynolds numbers ($Da=1e-6$)

A comparison between the Nusselt number for the two different Darcy numbers is shown in Fig. 18. The results show that the Nusselt number decreases as Darcy increases and vice versa. Generally we can say that, forced convection can be significantly enhanced by depositing porous substrate with low porosity and low Darcy numbers on heated walls.

The pressure drop is an important factor to be considered in the employment of porous media for the purpose of heat transfer enhancement. Heat transfer analysis cannot be completed without pressure drop analysis.

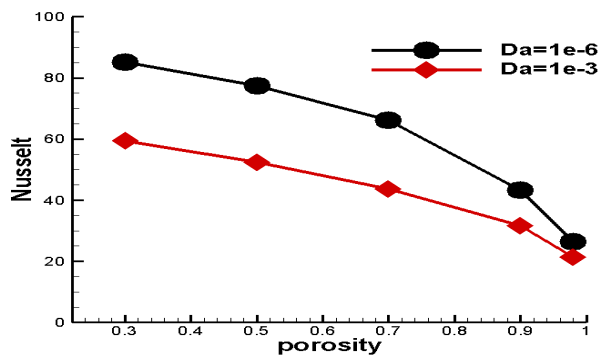


Fig. 18 Nusselt number versus porosity for two different Darcy numbers

Fig. 19 presents the numerical predictions of pressure drop as a function of porosity, for different Reynolds numbers. It is clearly seen that the highest values of pressure drop are obtained from lowest porosities and highest Re number. The pressure drop is inversely proportional to the porosity. The decrease in the porosity leads to increase in the friction between the fluid and the porous matrix which makes the pressure drop increasing. Also it can be seen that the effect of porosity becomes more significant when the Reynolds number is increased.

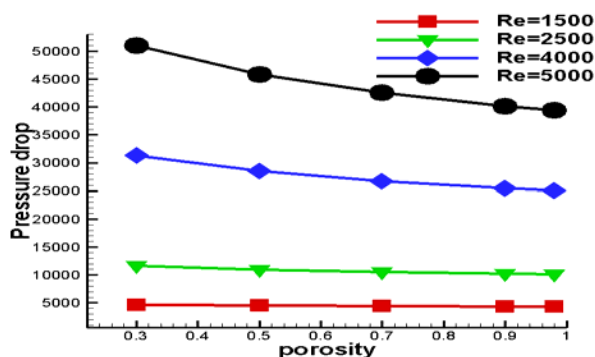


Fig. 19 Pressure drop versus porosity for different Reynolds numbers ($Da=1e-3$)

5 CONCLUSION

The present work numerically investigated the fluid flow behavior and heat transfer enhancements in a B-type cross sectioned pipe, which porous medium inserted on the bottom wall. The porous medium not only changes the condition of flow field which gives a thinner boundary layer, but also its heat conduction coefficient is generally higher than the ordinary fluid under investigation. Hence, introducing a porous medium into a channel efficiently improves the heat transfer performance of fluid flow in channel. From this analysis, it is clear that even for low flow rates,

significant improvement in heat transfer rate is achieved with the proposed porous layer in the B-Type section pipe. The highest increase in the Nusselt number of approximately 7.59 times, is obtained at $Re=5000$, $Da=1e-6$, $\gamma=0.3$, at the expense of the 2.26-fold increase in pressure drop.

6 NOMENCLATURE

d_p	particle diameter	x, y, z	Cartesian coordinates
Δp	pressure gradient	q''	heat flux
D_h	hydraulic diameter		
		Greek symbols	
Da	Darcy number (α/H^2)	α	permeability
$h(z)$	heat transfer coefficient	γ	porosity
H	height of the channel	ρ	fluid density
K	thermal conductivity	μ	viscosity
k	turbulence kinetic energy		
Nu	Nusselt number		
		Subscripts	
Re	Reynolds number ($\rho u_{in} D_h / \mu$)	f	fluid phase
T	temperature	s	solid phase
u	velocity along z-direction	eff	effective
U	magnitude of velocity vector	in	inlet

REFERENCES

- [1] Aliabbasi, R., Khayat, M., and Taiebi Rahni, M., "Numerical simulation of flow and forced convection heat transfer through a flattened pipe using porous material at the Core with constant heat flux", 4th National Conference of Mechanical Engineering, IAU of Khomeinishahr Branch, Nov. 2011.
- [2] Yang, Y., and Hwang, M., "Numerical simulation of turbulent fluid flow and heat transfer characteristics in heat exchangers fitted with porous media", International Journal of Heat and Mass Transfer, Vol. 52, April 2009, pp. 2956-2965.
- [3] Braga, E., and de Lemos, M., "Simulation of turbulent natural convection in a porous cylindrical annulus using a macroscopic two-equation model", International Journal of Heat and Mass Transfer, Vol. 49, July 2006, pp. 4340-4351.
- [4] Li, H. Y., Leong, K. C., Jin, L. W., and Chai, J. C., "Analysis of fluid flow and heat transfer in a channel with staggered porous blocks", International Journal of Thermal Sciences, Vol. 49, Feb. 2010, pp. 950-962.
- [5] Akansu, S., "Heat transfer and pressure drops for porous-ring turbulators in a circular pipe", Applied Energy, Vol. 83, June 2006, pp. 280-298.

- [6] Bogdan, I., Pavel, Abdulmajeed, and Mohamad, A., "An experimental and numerical study on heat transfer enhancement for gas heat exchangers fitted with porous media", *International Journal of Heat and Mass Transfer*, Vol. 47, August 2004, pp. 4939-4952.
- [7] Kaviany, M., "Laminar flow through a porous channel bounded by isothermal parallel plate", *International Journal of Heat and Mass Transfer*, Vol. 28, No. 4, 1985, pp. 851-858.
- [8] Alkam, M. K., and Al-Nimr, M. A., "Improving the performance of double-pipe heat exchangers by using porous substrates", *International Journal of Heat and Mass Transfer*, Vol. 42, Dec. 1999, pp. 3609-3618.
- [9] Shigeru, T., and Koichi, I., "Analysis of laminar dissipative flow and heat transfer in a porous saturated circular tube with constant wall heat flux", *International Journal of Heat and Mass Transfer*, Vol. 50, Feb. 2007, pp. 2406-2413.
- [10] Marafie, A., and Vafai, K., "Analysis of non-darcian effects on temperature differentials in porous media", *International Journal of Heat and Mass Transfer*, Vol. 44, March 2001, pp. 4401-4411.
- [11] Khaled, R. A., and Vafai, K., "Heat transfer enhancement through control of thermal dispersion effects", *International Journal of Heat and Mass Transfer*, Vol. 48, March 2005, pp. 2172-2185.
- [12] Mohamad, A. A., "Heat transfer enhancements in heat exchangers fitted with porous media part I: constant wall temperature", *International Journal of Thermal Sciences*, Vol. 42, May 2003, pp. 385-395.
- [13] Macedo, H. H., Costa, U. M. S., and Almeida, M. P., "Turbulent effects on fluid flow through disordered porous media", *Physica A*, Vol. 299, April 2001, pp. 371-377.
- [14] Silva, R. A., and de Lemos, M. J. S., "Turbulent flow in a channel occupied by a porous layer considering the stress jump at the interface", *International Journal of Heat and Mass Transfer*, Vol. 46, June 2003, pp. 5113-5121.
- [15] Pedras, M. H. J., and de Lemos, M. J. S., "Macroscopic turbulence modeling for incompressible flow through undeformable porous media", *International Journal of Heat and Mass Transfer*, Vol. 44, May 2001, pp. 1081-1093.
- [16] Silva, R. A., and de Lemos, M. J. S., "Turbulent flow in a composite channel", *International Communications in Heat and Mass Transfer*, Vol. 38, No. 8, 2011, pp 1019-1023.
- [17] Kaviany, M., "Principles of Heat Transfer in Porous Media", 2nd ed., Springer-Verlag, New York, 1995, Chaps. 3.
- [18] FLUENT 6.3 user's guide.